Parametric Design Study of Hybrid Steel Fibre Reinforced Concrete (SFRC) in Singapore Cut-and-Cover MRT Structures

ANG Wei Jian, GOH Kok Hun
Land Transport Authority, Singapore

ABSTRACT: The Singapore MRT construction industry saw its first successful implementation of Steel Fibre Reinforced Concrete (SFRC) permanent tunnel linings in Downtown Line (DTL) Stage 3, Contract C933 in 2011. Since then, SFRC permanent tunnel linings were widely adopted in other LTA projects such as Thomson East Coast Line (TEL), Circle Line Extension (CCLe), North East Line Extension (NELe) and Thomson-East Coast Line Extension (TELe). With the newly published Singapore Standard SS 674 in 2021, it is technically possible to extend the benefits of SFRC in permanent tunnel linings to Cut-and-Cover structures. This paper introduces the design concept presented in Singapore Standard SS 674 for hybrid SFRC structures which are reinforced with both steel fibres and steel reinforcement bars. Through a parametric study involving the re-design of critical hull elements in various LTA in-house design Cut-and-Cover MRT structures, the effectiveness of steel fibres and higher steel reinforcement yield strength in reducing the reinforcement quantity were also investigated and discussed in detail in this paper.

1 INTRODUCTION

Steel Fibre Reinforced Concrete (SFRC) tunnel linings have proliferated in the last decade in Singapore due to the numerous benefits it has to offer. As a result of the discrete and discontinuous nature of steel fibres, SFRC can limit the propagation of steel corrosion to enhance the durability of the structure. Furthermore, steel fibres in SFRC structure were found to be effective in bridging cracks and increasing the ductility of post-cracking behaviour (Peterson et al., 2009). This helps to reduce crack widths and restrict the ingress of deleterious agents, further improving durability. Against the backdrop of global warming, the environmental benefit of using SFRC is another important consideration. A recent study on Grand Paris Express project (Wallis, 2022) revealed that SFRC tunnel linings are up to 300% more beneficial to the environment than typical reinforced concrete (RC) tunnel linings in part due to the lower carbon emission associated with steel fibres production. Thus, the use of SFRC would reduce carbon footprint, and support a more sustainable and carbon constrained construction.

Noting the various advantages of SFRC, there is keen interest to expand its application beyond tunnel linings, and use it for other underground structures such as Cut-and-Cover structures. However, the design of SFRC tunnel linings is based on unreinforced and uncracked sections (Goh and Wen, 2017, Shi et al., 2021) of the prevailing RC design codes, as there were no national codes of practice to guide the design of fibre reinforced concrete structures. This is possible for circular bored tunnels, as the predominant loads under hoop action would be axial and compressive in nature. However, the application of SFRC for other underground Cut-and-Cover structures are limited, as these are non-circular and are typically designed with significant bending reinforcements to resist cracking within an allowable limit.

In June 2021, Singapore Standard SS 674 “Fibre concrete – Design of fibre concrete structures” was first published to provide guidance on fibre concrete structures design. The introduction of SS 674

allows designers to characterise the performance of fibre reinforced concrete and design "hybrid SFRC structures" which are reinforced with both steel fibres and steel reinforcement bars (rebars). This creates an opportunity to capitalise on SFRC in non-circular underground structures.

2 DESIGN CONCEPT OF HYBRID SFRC STRUCTURE IN ACCORDANCE WITH SS 674

A design is guided by two main limit states – Serviceability Limit State (SLS) and Ultimate Limit State (ULS). SS 674 (2021) presents design methodologies to account for the beneficial effects of steel fibres in reducing crack width and improving bending moment capacity of hybrid SFRC structures, to fulfil SLS and ULS requirements respectively. These design checks are necessary to determine the required quantity of bending reinforcements in hybrid SFRC structures.

2.1 Ductile post-cracking behaviour of SFRC

SFRC and plain concrete differ greatly in their post-cracking behaviours as illustrated in Figure 1. Plain concrete reaches peak stress and cracks at a small tensile strain. Once cracked, the stress in concrete drops sharply to zero. Hence, in typical RC design, concrete is assumed to have zero tensile strength. However, SFRC retains residual tensile strength even after it reaches peak tensile stress and cracks.

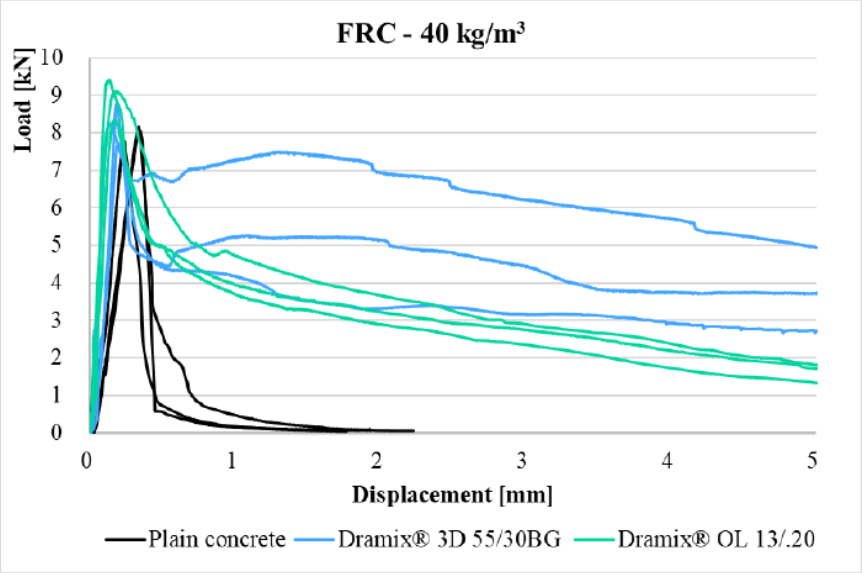

* The green and blue curves represent the load-displacement behaviour of SFRC with different Dramix® steel fibres.

Figure 1. Load-displacement curves for plain concrete and steel fibre reinforced concrete (Marcalikova et al., 2020)

The ductile post-cracking behaviour exhibited by SFRC is also described in Figure 2. The higher post-cracking tensile strength corresponding to a small displacement ($f_{R,1}$) is commonly associated with SLS design where SFRC tensile strain is also small. Conversely, the lower post-cracking tensile strength corresponding to a much larger displacement ($f_{R,3}$) is used in ULS design where SFRC tensile strain is also larger. For the rest of the paper, $f_{R,1}$ and $f_{R,3}$ will be termed as the "SFRC tensile strength in SLS" and "SFRC tensile strength in ULS" respectively.

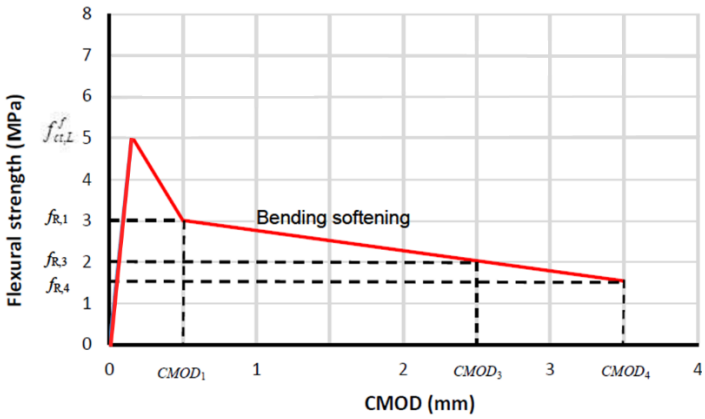

Symbol	Definition
$f_{R,1}$	Characteristic residual flexural tensile strength corresponding to CMOD of 0.5mm ("SFRC tensile strength in SLS")
$f_{R,3}$	Characteristic residual flexural tensile strength corresponding to CMOD of 2.5mm ("SFRC tensile strength in ULS")
$f_{R,4}$	Characteristic residual flexural tensile strength corresponding to CMOD of 3.5mm

Figure 2. Plot of flexural strength against crack mouth opening displacement (CMOD) for fibre concrete (Adapted from SS 674, 2021)

2.2 Effect of Fibre Orientation on design SFRC tensile strength

According to Singh (2017), the fibre orientation has a significant effect on design SFRC tensile strength. The use of steel fibres is more effective in thin horizontal members such as slabs where the preferential fibre orientation is along the principal directions of the tensile stress trajectories. Such a fibre orientation is favourable as the fibres are more readily activated to resist tension, leading to higher design SFRC tensile strength.

In SS 674 (2021), the fibre orientation factor (n_f) is introduced to account for the effect of fibre orientation. For local practice, n_f is taken as 1 for horizontally cast members, such as slabs and tunnel segments with width-to-thickness ratio larger than five, because the preferential fibre orientation is favourable. For other cases, n_f is taken as 0.5 to halve the design SFRC tensile strength.

2.3 Serviceability Limit State (SLS) crack width check

With reference to SS 674 (2021), BS EN 1992-1-1 (2004) and NA to SS EN 1992-1-1 (2008), the equations for crack width calculations in RC structure and hybrid SFRC structure are compiled in Table 1.

Table 1. Comparison of equations for crack width calculations between RC structure (BS EN 1992-1-1, 2004 and Tan, 2017) and hybrid SFRC structure (SS 674, 2021)

Equations for crack width calculations	
RC Structure	**Hybrid SFRC Structure**
Crack width, w_k	
$w_k = S_{r,max}(\varepsilon_{sm} - \varepsilon_{cm})$ (1)	
Maximum crack spacing, $S_{r,max}$	
$S_{r,max} = k_3 \times c + k_1 \times k_2 \times k_4 \times \frac{\phi}{\rho_{p,eff}}$ (2)	$S_{r,max} = k_3 \times c + k_1 \times k_2 \times k_4 \times (1 - k_f) \times \frac{\phi}{\rho_{p,eff}}$ (3)
Strain Difference between rebar and concrete, $\varepsilon_{sm} - \varepsilon_{cm}$	
$\varepsilon_{sm} - \varepsilon_{cm} = \frac{\sigma_s - k_t \frac{f_{ct,eff}}{\rho_{p,eff}}(1 + \alpha_e \rho_{p,eff})}{E_s} \geq 0.6 \frac{\sigma_s}{E_s}$ (4)	$\varepsilon_{sm} - \varepsilon_{cm} = \frac{(1 - k_f)(\sigma_{s,fict} - k_t \frac{f_{ct,eff}}{\rho_{p,eff}}(1 + \alpha_e \rho_{p,eff}))}{E_s} \geq 0.6(1 - k_f)\frac{\sigma_{s,fict}}{E_s}$ (5)

Table 1 reveals a key difference – the k_f term only appears in the crack width equations for hybrid SFRC structure. The k_f term is defined as the ratio between the SFRC tensile strength in SLS and the concrete tensile strength:

$$k_f = \frac{f_{ftd,R1}}{f_{ctm}} \leq 1.0 \tag{6}$$

Noting the k_f term is less than unity, the calculated crack width will always be less for hybrid SFRC structure. Hence, the beneficial effect of the steel fibres in hybrid SFRC structure in bridging cracks is accounted for with these equations.

2.4 Ultimate Limit State (ULS) bending moment capacity check

For the design of hybrid SFRC structure in ULS, SS 674 (2021) proposed three possible stress distributions with non-zero tensile stress block as shown in Figure 3. This departs from typical RC design in which cracked concrete is assumed to have zero tensile strength. By allowing the cracked SFRC to resist tension, SS 674 has accounted for the improvement in section capacity due to the ductile post-cracking behaviour in hybrid SFRC structure.

For the proposed stress distributions to be valid, it is worth noting that the SFRC tensile strain should not exceed the tensile strain limit ε_{ftu}. This constraint typically leads to a marginal improvement in the ULS capacity of SFRC.

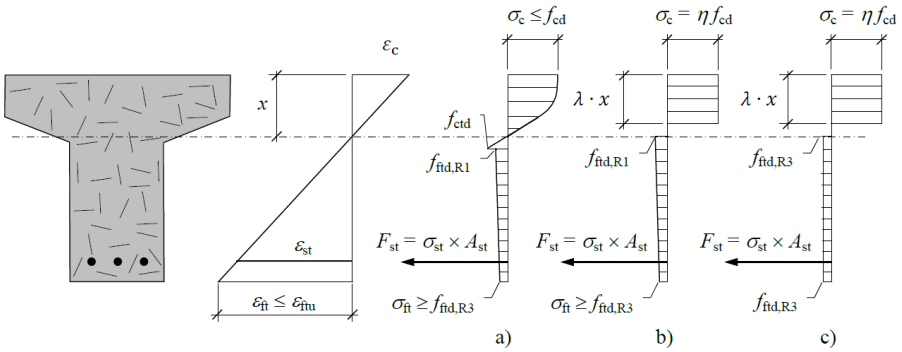

Figure 3. Possible range of stress distributions in hybrid SFRC structure (SS 674, 2021)

Apart from steel fibres, the rebar yield strength will also affect the ULS bending moment capacity. The effectiveness of higher rebar yield strength in improving the structural capacity will also be explored in this study.

3 OVERVIEW OF DESIGN ASSUMPTIONS AND VARIABLES ADOPTED IN PARAMETRIC STUDY

The benefits of steel fibres and higher rebar yield strength were investigated in this study through the re-design of critical hull elements in MRT structures – roof slabs, base slabs and diaphragm walls of ongoing projects, such as the upcoming NELe Punggol Coast Station and crossover tunnels and the TELe Cut-and-Cover Launch Shaft. In this study, the design forces and design parameters followed the values in the approved QP(D) design report.

3.1 Definition of independent variables in parametric study

This sub-section introduces the three main design variables for this parametric study – the rebar yield strength (f_{yk}) as well as the SFRC tensile strength in SLS and ULS ($f_{R,1}$ and $f_{R,3}$ respectively).

It is noted that rebar yield strength of 500 MPa is mostly used in underground construction industry in Singapore. Conversely, BS EN 1992-1-1 (2004) has advised an upper limit of 600 MPa for rebar yield strength, above which design rules in Eurocode 2 are invalid. Hence, the rebar yield strength of 500 MPa and 600 MPa were selected for this study.

Separately, $f_{R,1}$ value of 3 MPa and 5 MPa were chosen for this parametric study as they fall within the 2.8 - 5.2 MPa $f_{R,1}$ range as specified in past LTA projects and overseas tunnel projects shown in Table 2. In view of the $f_{R,4}$ range of 1.4 MPa to 3.0 MPa in Table 2, the highest value of 3 MPa is selected for $f_{R,3}$ in order to maximise enhancement to ULS section capacity.

Table 2. Summary of target $f_{R,1}$ and $f_{R,4}$ for precast SFRC tunnel segments in past LTA projects (Wei et al., 2018 and Shi et al., 2021) and overseas tunnel projects (International Tunnel Association, 2016)

	DTL C933 Tunnel	TEL T206 Tunnel	TEL T207 Tunnel	NELe Tunnel	Hobson Bay Sewer Tunnel	Southall to Harefield Gas Pipeline	Pista Nueva Malaga High Speed Rail Tunnel
$f_{R,1}$ (MPa)	2.8	5.0	5.2	2.8	3.5	5.0	5.0
$f_{R,4}$ (MPa)	1.4	2.0	1.7	1.4	3.0	2.4	2.9

4 RESULTS OF PARAMETRIC STUDY BASED ON C715 CUT-AND-COVER TUNNEL

A parametric study was conducted to examine the effect of steel fibres and rebar yield strength on SLS crack width crack and ULS bending moment capacity check. Results from C715 Cut-and-Cover Tunnel will be reviewed in sub-section 4.1—4.3. As shown in Figure 4, C715 Cut-and-Cover Tunnel is part of NELe works and can be found in Zone 1, immediately after the existing NE17 Overrun Tunnel. A typical cross section is presented in Figure 5.

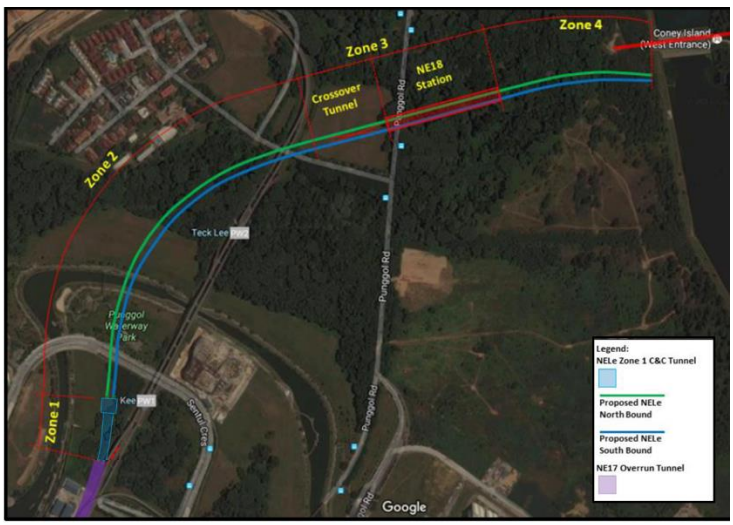

Figure 4. Location of C715 Cut-and-Cover Tunnel

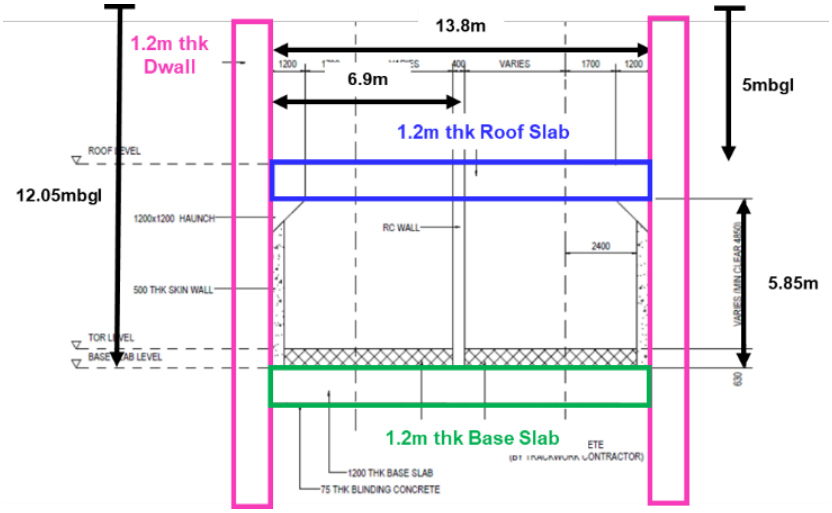

Figure 5. Typical cross section of C715 Cut-and-Cover Tunnel

The ULS and SLS bending moment envelopes for slabs and walls in C715 Cut-and-Cover Tunnel are shown in Figure 6 and 7 respectively. The design sections for the roof slab (RS-1), base slab (BS-1) and diaphragm wall (DW-1) have also been identified.

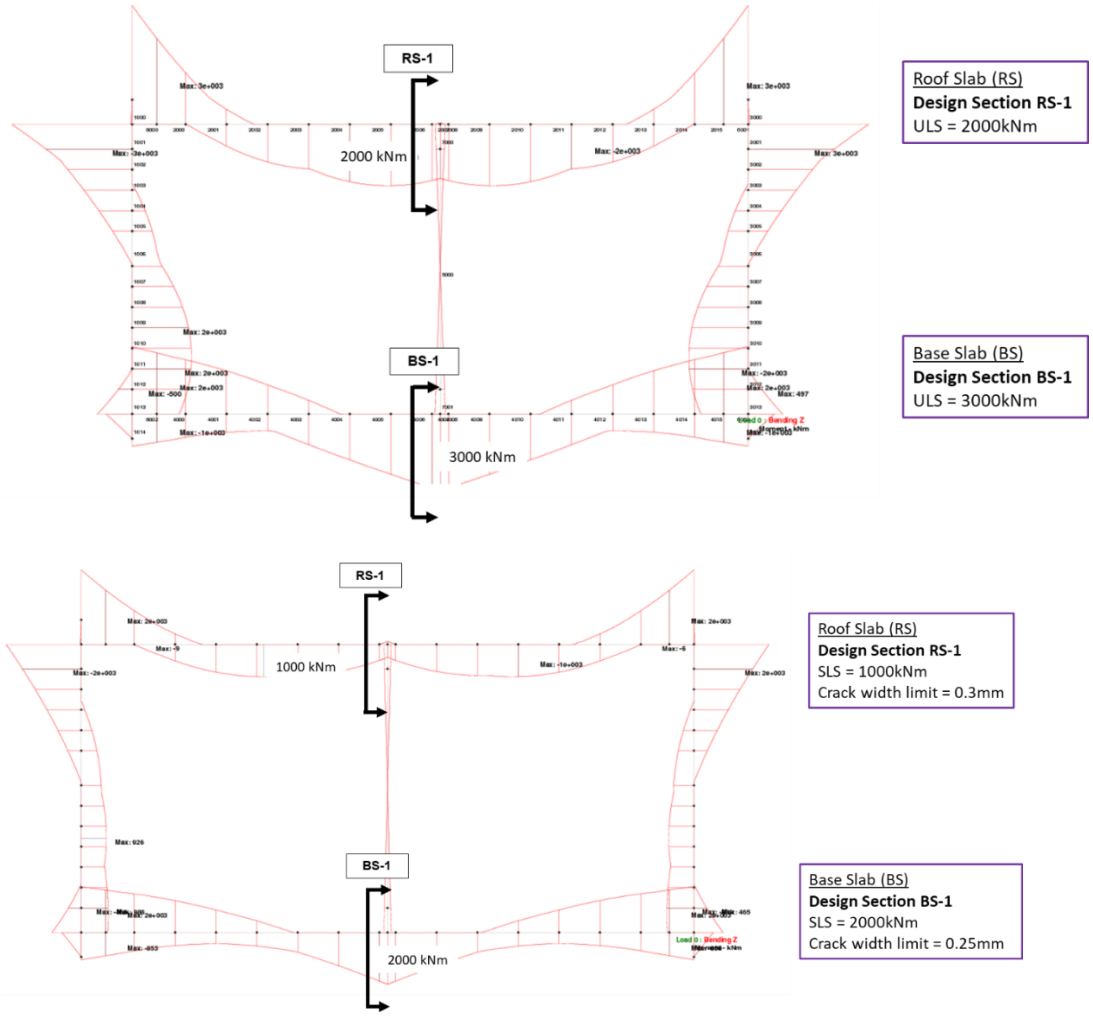

Figure 6. ULS and SLS bending moment envelope for slab elements

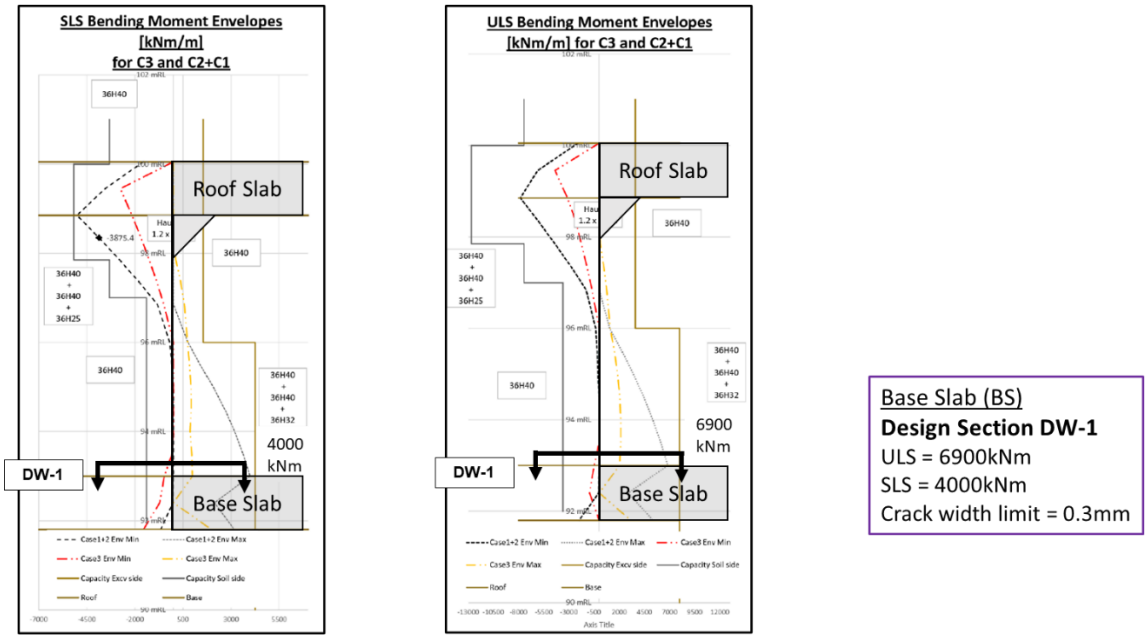

Figure 7. ULS and SLS bending moment envelope for wall elements

4.1 Effect of steel fibres on SLS crack width check

This sub-section explores the effect of steel fibres on SLS crack width check by re-designing sections according to the cases listed in Table 3.

Table 3. Summary of cases to demonstrate the effect of steel fibres on SLS crack width check

Case Name	Material	SFRC Tensile Strength in SLS $f_{R,1}$ (MPa)	SLS Rebar Quantity
Base Case	RC	-	Optimised
Case A1	Hybrid SFRC (RC + Fibres)	3	Same as Base Case
Case A2	Hybrid SFRC (RC + Fibres)	3	Optimised
Case A3	Hybrid SFRC (RC + Fibres)	5	Optimised

As seen in Table 3, Base Case adopts a typical RC design with no fibres. The rebar quantity in Base Case has also been optimised, meaning that the minimum rebar amount that is required to resist the design forces has been provided. For Cases A1 to A3, a design of hybrid SFRC structure is considered with varying SFRC strength. For Case A1, the rebar quantity is kept the same as that in Base Case to study the beneficial effect of steel fibres on crack width reduction. However, for Case A2 and A3, the rebar quantity is optimised based on the SLS requirements so rebar savings can be realised with the addition of steel fibres. The results for the re-designed sections are shown in Table 4.

Table 4. Effect of steel fibres on SLS crack width

Design Section	Case Name	Material	SFRC Tensile Strength in SLS $f_{R,1}$ (MPa)	SLS Rebar Quantity	SLS Crack Width (mm)
RS-1 in Roof Slab	Base Case	RC	-	1 layer of H32-150	0.255
	Case A1	Hybrid SFRC (RC + Fibres)	3	1 layer of H32-150	0.119
	Case A2	Hybrid SFRC (RC + Fibres)	3	1 layer of H25-150	0.218
	Case A3	Hybrid SFRC (RC + Fibres)	5	1 layer of H16-150	0.255
BS-1 in Base Slab	Base Case	RC	-	1 layer of H40-150 & 1 layer of H25-150	0.250
	Case A1	Hybrid SFRC (RC + Fibres)	3	1 layer of H40-150 & 1 layer of H25-150	0.125
	Case A2	Hybrid SFRC (RC + Fibres)	3	1 layer of H40-150	0.183
	Case A3	Hybrid SFRC (RC + Fibres)	5	1 layer of H25-150	0.225
DW-1 in Dwall	Base Case	RC	-	2 layers of H40-150 & 1 layer of H32-150	0.287
	Case A1	Hybrid SFRC (RC + Fibres)	3	2 layers of H40-150 & 1 layer of H32-150	0.214
	Case A2	Hybrid SFRC (RC + Fibres)	3	2 layers of H40-150	0.262
	Case A3	Hybrid SFRC (RC + Fibres)	5	1 layer of H40-150 & 1 layer of H25-150	0.287

By comparing Base Case and Case A1 for the roof slab, base slab and diaphragm wall sections in Table 4, the addition of steel fibres resulted in a significant drop in the crack width. An approximate 25% and 50% reduction in crack width were observed in the wall and slab elements respectively. This difference can be explained with the fibre orientation factor (n_f) which is set as 1 for horizontally cast slabs and 0.5 for vertically cast diaphragm walls. This results in a smaller design SFRC strength for wall elements, leading to less reduction in crack width.

A comparison of Base Case with Case A2 and Case A3 revealed that the addition of steel fibres can result in significantly lower rebar quantity while satisfying the allowable crack width limit. The higher the SFRC tensile strength ($f_{R,1}$), the greater the reduction in rebar quantity – this holds true for both wall and slab elements.

It is important to note that the calculated crack width can be much lower than the allowable crack width limit, even when the rebar quantity is optimised. This is due to the availability of rebars only in standard diameters. With this constraint, it is very challenging to obtain the most optimised rebar quantity for design capacity to match design force exactly.

4.2 Effect of steel fibres on ULS bending moment capacity check

This sub-section explores the effect of steel fibres on ULS bending moment capacity check by re-designing critical sections according to the cases listed in Table 5.

Table 5. Summary of cases to demonstrate the effect of steel fibres on ULS bending moment capacity check

Case Name	**Material**	**SFRC Tensile Strength in ULS $f_{R,3}$ (MPa)**	**ULS Rebar Quantity**
Base Case	RC	-	Optimised
Case B1	Hybrid SFRC (RC + Fibres)	3	Optimised

As seen in Table 5, only steel fibres are considered for Case B1. The rebar quantity for both cases has been optimised. The results for the re-designed sections are shown in Table 6.

Table 6. Effect of steel fibres on ULS bending moment capacity check

Design Section	**Case Name**	**Material**	**SFRC Tensile strength in ULS $f_{R,3}$ (MPa)**	**ULS Rebar Quantity**	**ULS Bending Moment Capacity (kNm)**
RS-1 in Roof Slab	Base Case	RC	-	1 layer of H32-150	2493
	Case B1	Hybrid SFRC (RC + Fibres)	3	1 layer of H32-150	2501
BS-1 in Base Slab	Base Case	RC	-	1 layer of H40-150	3754
	Case B1	Hybrid SFRC (RC + Fibres)	3	1 layer of H40-150	3772
DW-1 in Dwall	Base Case	RC	-	2 layers of H40-150 & 1 layer of H25-150	6904
	Case B1	Hybrid SFRC (RC + Fibres)	3	2 layers of H40-150 & 1 layer of H25-150	6952

With reference to Table 6, the increase in ULS bending moment capacity due to steel fibres is less than 1%. This is due to the inadequacy of SFRC to resist tension beyond the tensile strain limit ε_{ftu}. Owing to the negligible contribution of steel fibres to the section capacity, the rebar amount cannot be reduced further in Case B1 as the ultimate moment capacity is still largely provided by the main rebars.

4.3 Effect of higher rebar yield strength on ULS bending moment capacity check

This sub-section explores the effect of higher rebar yield strength on ULS bending moment capacity check by re-designing critical sections according to the cases listed in Table 7.

Table 7. Summary of cases to demonstrate the effect of higher rebar yield strength on ULS bending moment capacity check

Case Name	Material	Rebar Yield Strength f_{yk} (MPa)	ULS Rebar Quantity
Base Case	RC	500	Optimised
Case C1	RC	600	Same as Base Case
Case C2	RC	600	Optimised

As seen in Table 7, the key difference between Base Case with Case C1 and Case C2 is the rebar yield strength. For Case C1, the rebar quantity is kept the same as that in Base Case to study the improvement of ULS capacity by using higher rebar yield strength. However, for Case C2, the rebar quantity is optimised to illustrate the rebar savings attributed to the increase in rebar yield strength. The results for the re-designed sections are shown in Table 8.

Table 8. Effect of higher rebar yield strength on ULS bending moment capacity check

Design Section	Case Name	Material	Rebar Yield Strength f_{yk} (MPa)	ULS Rebar Quantity	ULS Bending Moment Capacity (kNm)
RS-1 in Roof Slab	Base Case	RC	500	1 layer of H32-150	2493
	Case C1	RC	600	1 layer of H32-150	2916
	Case C2	RC	600	1 layer of H25-125	2182
BS-1 in Base Slab	Base Case	RC	500	1 layer of H40-150	3754
	Case C1	RC	600	1 layer of H40-150	4361
	Case C2	RC	600	1 layer of H32-150	3451
DW-1 in Dwall	Base Case	RC	500	2 layers of H40-150 & 1 layer of H25-150	6904
	Case C1	RC	600	2 layers of H40-150 & 1 layer of H25-150	7341
	Case C2	RC	600	2 layers of H40-150	7009

By comparing Base Case and Case C1 in Table 8, the increase in steel grade of rebars resulted in an improvement in the ULS bending moment capacity. An approximate 6% and 16% increase in section capacity were observed in wall and slab elements respectively. This difference can be reconciled by examining the rebar arrangement. The slab elements only need one layer of rebar to achieve the desired ULS capacity. However, the required rebar quantity in the wall element is larger due to higher design forces, and has to be arranged in multiple layers. The percentage reduction in lever arm, arising from the increase in rebar yield strength, will be larger for each successive rebar layer. Hence, the increase in rebar yield strength has diminishing returns on the section capacity for each rebar layer introduced, causing the higher rebar yield strength to be less effective in the wall element. Nonetheless, it is shown in Case C2 that higher rebar yield strength allows for a reduction in the required rebar quantity for all the elements studied.

Also, rebar yield strength has no effect on SLS capacity. Based on BS EN 1992-1-1 (2004), crack width depends on the rebar working stress which is much smaller than the rebar yield strength. Thus, the improvement in yield strength does not reduce crack width further, and hence no benefit in reducing the amount of rebars required in the SLS design.

5 Combined effects of steel fibres and rebar yield strength on SLS and ULS design checks

The effect of steel fibres and rebar yield strength have been studied independently in sub-section 4.1 – 4.3. This section investigates the combined effect of steel fibres and rebar yield strength on rebar quantity by re-designing critical sections according to the design scenarios listed in Table 9. For all design scenarios, a concrete grade (f_{ck}) of C35/45 is adopted.

Table 9. Summary of design scenarios to demonstrate the effect of steel fibres and rebar yield strength on rebar quantity

Design Scenario (DS)	Description
Base DS	RC structure (f_{ck}=35 MPa) with rebar (f_{yk}=500 MPa) and without steel fibres
DS 1	Hybrid SFRC structure (f_{ck}=35 MPa) with rebar (f_{yk} =500 MPa) and steel fibres ($f_{R,1}$=3 MPa)
DS 2	Hybrid SFRC structure (f_{ck}=35 MPa) with rebar (f_{yk} =500 MPa) and steel fibres ($f_{R,1}$=5 MPa)
DS 3	RC structure (f_{ck}=35 MPa) with rebar (f_{yk}=600 MPa) and without steel fibres
DS 4	Hybrid SFRC structure (f_{ck}=35 MPa) with rebar (f_{yk} =600 MPa) and steel fibres ($f_{R,1}$=3 MPa)

As seen in Table 9, only two independent variables are examined: SFRC tensile strength in SLS ($f_{R,1}$) and rebar yield strength (f_{yk}). Noting the negligible improvement in the ULS section capacity when steel fibres are added, SFRC tensile strength in ULS ($f_{R,3}$) is no longer considered.

5.1 Summary of results based on C715 Cut-and-Cover Tunnel

The results for the re-designed sections in C715 Cut-and-Cover Tunnel are shown in Figure 8a, 8b and 8c. As structure design has to satisfy the requirements in both limit states, the final rebar quantity is given as an envelope of the rebar needed to fulfil SLS and ULS requirements. In Figures 8a to 8c, the final rebar quantity for each design scenario (DS) has been boxed up in red. It is also important to note that the rebar quantity for each DS has been optimised, and the minimum rebar quantity is provided.

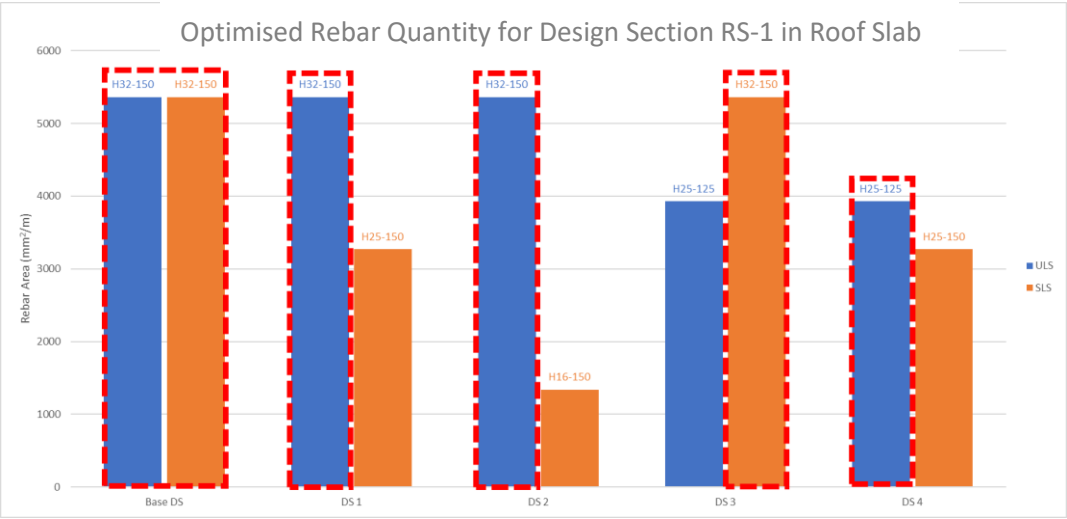

Figure 8a. Graph showing optimised ULS and SLS rebar quantity for design section RS-1 for each design scenario (DS)

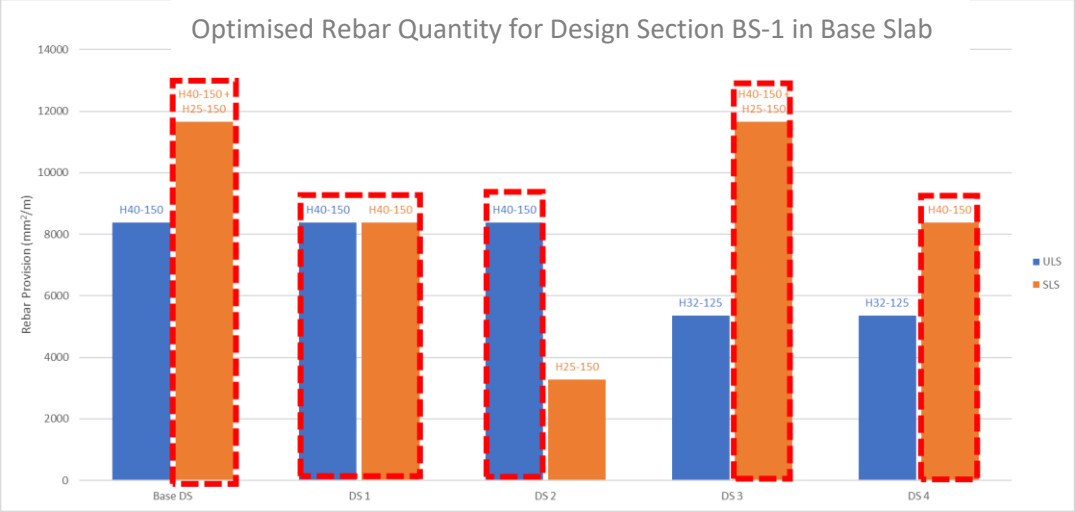

Figure 8b. Graph showing optimised ULS and SLS rebar quantity for design section BS-1 for each design scenario (DS)

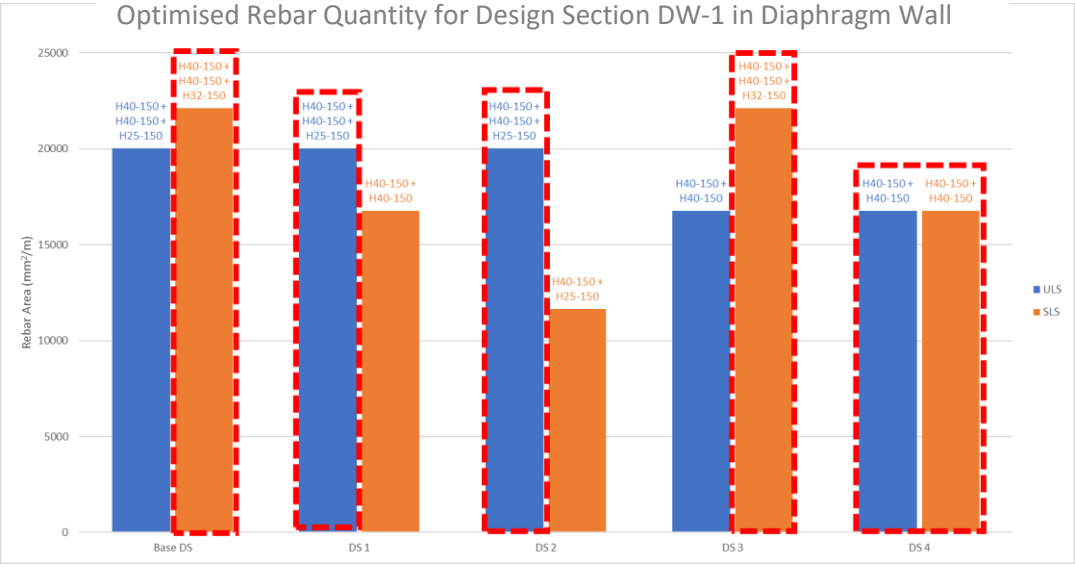

Figure 8c. Graph showing optimised ULS and SLS rebar quantity for design section DW-1 for each design scenario (DS)

Generally, it is observed that the final rebar quantity in DS 1 is less than that in Base DS, and the rebar reduction ranges from 10% to 30%. This illustrates the effectiveness of steel fibres in reducing the final rebar quantity. As SLS requirements govern in the Base DS, a reduction in SLS rebar quantity brought about by the addition of steel fibres in DS 1 will also lessen the final rebar quantity. However, as seen in Figure 8a, this observation does not hold true for the roof slab element due to its low design forces.

Another observation is that the final rebar quantity in DS 2 is always equal to that in DS 1. This suggests that there may be limited benefit in reducing rebar by over-specifying SFRC tensile strength in SLS ($f_{R,1}$) beyond 3 MPa. SLS requirements no longer govern with a $f_{R,1}$ value of 3 MPa in DS 1. Further reduction in SLS rebar quantity brought about by a higher $f_{R,1}$ value in DS 2 will not reduce the final rebar required.

It is also noted that the final rebar quantity in DS 3 is always equal to that in Base DS, and suggests that it is futile to just adopt a higher rebar yield strength (f_{yk}) if ULS requirements do not govern the design. As shown in the Base DS, a reduction in ULS rebar quantity brought about by the higher rebar yield strength in DS 3 will not reduce the final rebar quantity which is still governed by SLS requirements.

Lastly, it is important to highlight that the combined use of steel fibres and a higher rebar yield strength in DS 4 can sometimes result in the minimum final rebar quantity. This is seen in Figure 8a and 8c, revealing the synergistic interaction between the two proposed enhancements to typical RC design.

5.2 Summary of results based on all case studies

As DS 1 and DS 4 findings are more significant, the design sections corresponding to the Base DS, DS 1 and DS 4 were compared for all the remaining design sections from the case studies. The most optimised design scenario with least final rebar quantity was determined for each of the 31 slab design sections and 20 diaphragm wall design sections, as shown in Figure 9. Further information on the case studies and the design sections can be found in appendices A and B. The results for all the design sections are also compiled in appendix C.

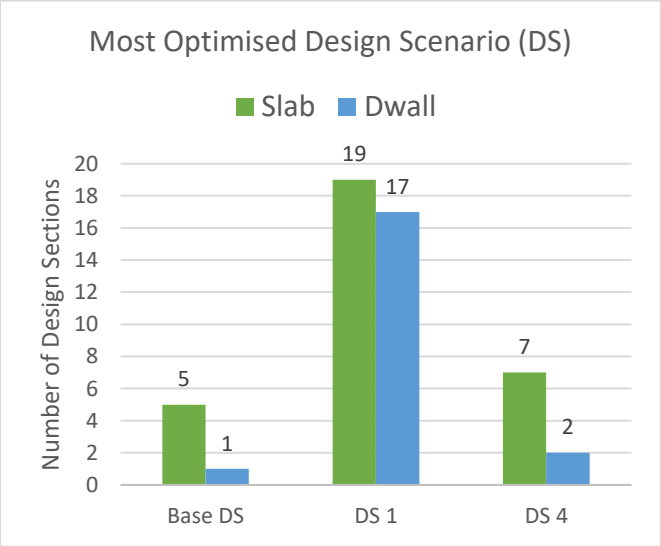

Design Scenario (DS)	Description
Base DS	RC structure (f_{ck}=35 MPa) with rebar (f_{yk}=500 MPa) and without steel fibres
DS 1	Hybrid SFRC structure (f_{ck}=35 MPa) with rebar (f_{yk} =500 MPa) and steel fibres ($f_{R,1}$=3 MPa)
DS 4	Hybrid SFRC structure (f_{ck}=35 MPa) with rebar (f_{yk} =600 MPa) and steel fibres ($f_{R,1}$=3 MPa)

Figure 9. Chart showing the most optimised design scenario with least final rebar quantity

As seen in Figure 9, DS 1 through using steel fibres alongside with G500 main rebars, has the highest occurrence of design sections with least final rebar quantity for both slab and wall elements, and presents the best opportunity for design optimisation. This is consistent with the observation made in sub-section 5.1 that steel fibres are effective in reducing the final rebar quantity.

It is also observed that DS 4 is rarely the most optimised. This shows that when steel fibres are already added, a higher rebar yield strength is redundant. As design sections for underground MRT tunnels are mostly governed by SLS requirements, the improvement in ULS section capacity brought about by higher rebar yield strength is unlikely to reduce rebar quantity. Furthermore, a higher rebar yield strength can be counter-productive as it will result in longer rebar anchorage and lapping length.

6 CONCLUSION

Until the advent of local standard SS 674, hybrid SFRC structures, which are reinforced with both steel fibres and rebars, have been used primarily in circular bored tunnels with limited application in non-circular structures. Through a parametric study, the paper investigated the effects of steel fibres and higher rebar yield strength in non-circular tunnel structures with reference to SS 674 (2021) and BS EN 1992-1-1 (2004). The key findings are:

- Steel fibres are effective in enhancing crack width control in SLS, but have displayed minimal improvement to ULS capacity. This is due to the inadequacy of SFRC to resist tension beyond the tensile strain limit ε_{ftu}.
- Higher rebar yield strength can improve ULS capacity significantly, but has no use in reducing SLS crack width. The higher rebar yield strength associated with higher steel grade does not affect crack width which depends on the rebar working stress.
- Arguably, combining both enhancements to typical RC design – steel fibres and higher rebar yield strength – will result in maximum rebar reduction.
- However, further investigation involving the re-design of critical hull elements in various LTA in-house design Cut-and-Cover MRT structures has demonstrated that a reduction in rebar quantity is more significant by using steel fibres for crack width control. The use of high steel grade is not useful as the section design is typically governed by SLS requirements.

It is important to note that these findings were obtained by following the design methodology in the code. Assumptions have been made about the values of modification factors such as the fibre orientation factor. The influence of construction challenges on fibre distribution within cast in-situ structures would also need to be investigated. The next step of the study would be to conduct material tests and scale model tests to calibrate these modification factors to accurately capture the effect of fibre orientation and fibre distribution in the design of hybrid SFRC structures.

7 REFERENCES

BS EN 1992-1-1. (2004) *Eurocode 2 – Design of concrete structures – Part 1-1: General rules and rules for buildings.*

Goh, K. H. and Wen, D. (2017) Design Practice On tunnels & Tunnelling in Singapore – Current State & Future Trends. *GeoSS 10th Anniversary Conference on A Decade of Geotechnical Advances, 30 Nov to 1 Dec 2017, Singapore.*

International Tunnel Association. (2016) ITAtech Guidelines for Precast Fibre Reinforced Concrete Segmenets – Vol. 1: Design Aspects, ITAtech Activity Group Support.

LTA Civil Design Criteria. (2019) Civil Design Criteria for Road and Transit Systems, Sep 2019, Land Transport Authority, Singapore.

Marcalikova, Z., Cajka, R., Bilek, V., Bujdos, D. and Sucharda, O. (2020) Determination of Mechanical Characteristics for Fiber-Reinforced Concrete with Straight and Hooked Fibers. *Crystals*. 10(6):545.

NA to SS EN 1992-1-1. (2008) *Singapore National Annex to Eurocode 2: Design of concrete structures – Part 1-1: General rules and rules for buildings.*

Peterson, G. L., Wen, D., Poh, J. and Tan, K. H. (2009) Structural testing of steel fibre reinforced concrete (SFRC) tunnel lining segments in Singapore. *WTC 2009.*

Singh, H. (2017) *Steel Fiber Reinforced Concrete: Behavior, Modelling and Design*. Singapore, Springer Nature.

Shi, W., Zou, M., Goh, K. H. and Zhang, B. (2021) Use of Steel Fibre Reinforced Concrete Linings in North East Line Extension MRT Project. *Underground Singapore Conference 2021.*

SS 674. (2021) *Fibre concrete – Design of fibre concrete structures.*

Tan, K. H. (2017*) Serviceability Limit States – Stress Limitation & Crack Control.* [Lecture] CE5510 Advanced Structural Concrete Design. National University of Singapore.

Wallis, S. (2022) A leap forward for SFRC segmental linings in France. *TunnelTalk*.

Wei, X., Su, T. and Goh, K. H. (2018) Design consideration and Application of Steel Fiber Reinforced Concrete (SFRC) in Singapore MRT Tunnels. *Underground Singapore Conference 2018.*

APPENDIX A

Typical cross-section of case studies

Figures A1 to A5 show the typical cross sections of the case studies considered:

- C715 Cut-and-Cover Tunnel
- TELe Cut-and-Cover Launch Shaft
- C717 Cut-and-Cover Overrun Tunnel
- C717 Cut-and-Cover Crossover Tunnel
- NELe Punggol Coast Station

Information on the structure geometry and overburden depth are also shown.

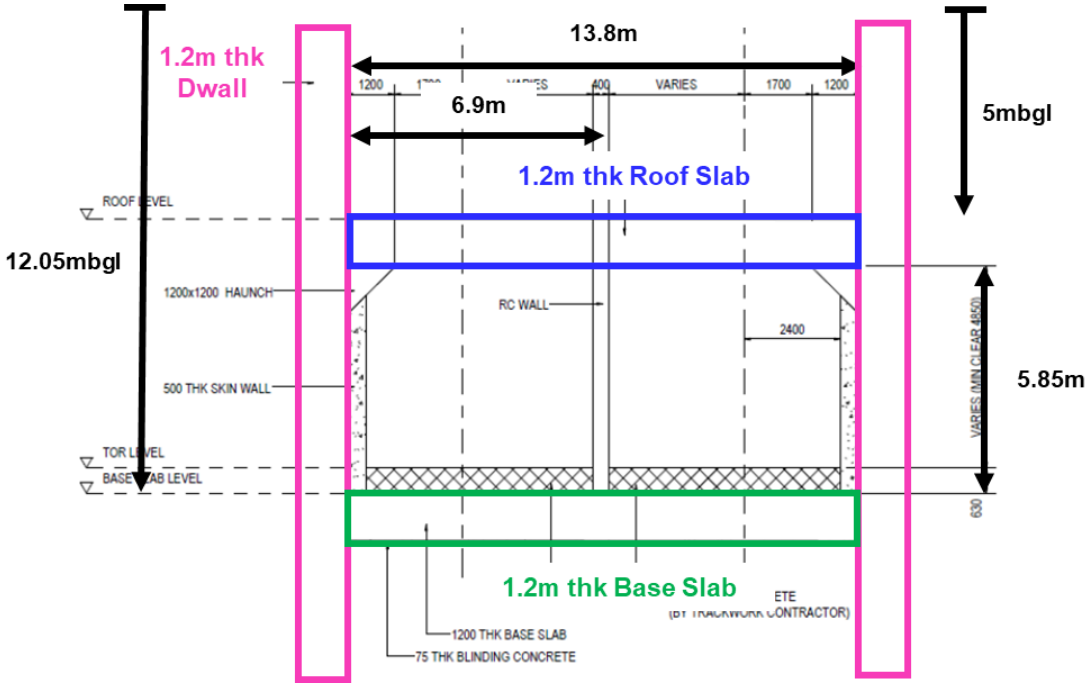

Figure A1. Typical cross section of C715 Cut-and-Cover Tunnel

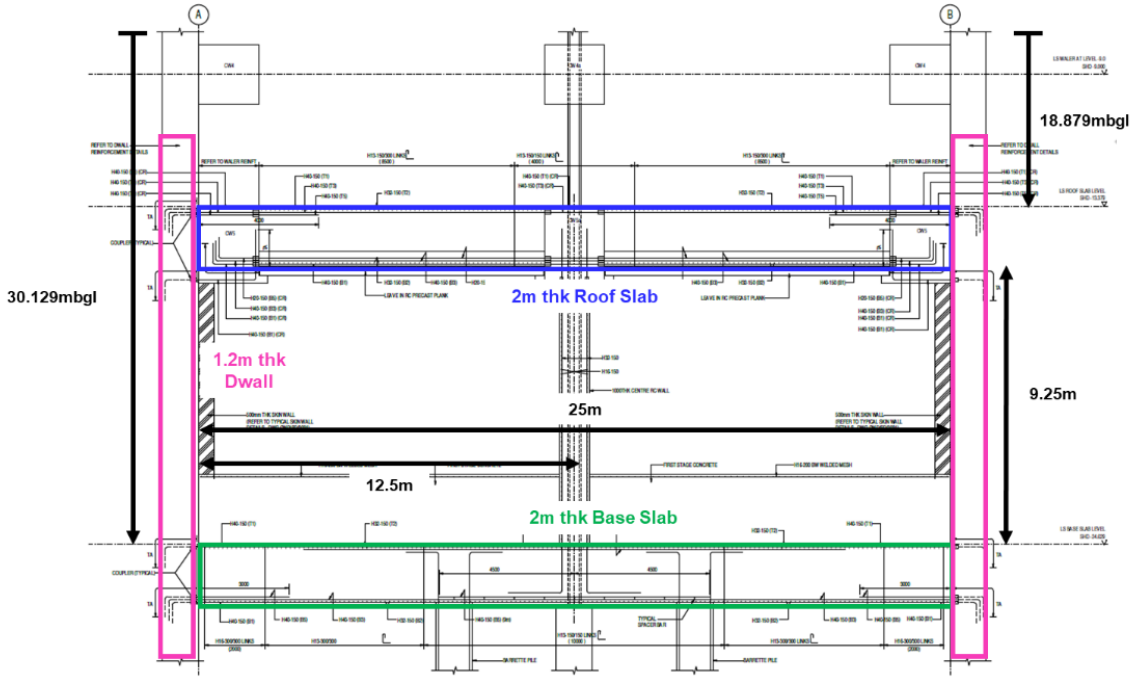

Figure A2. Typical cross section of TELe Cut-and-Cover Launch Shaft

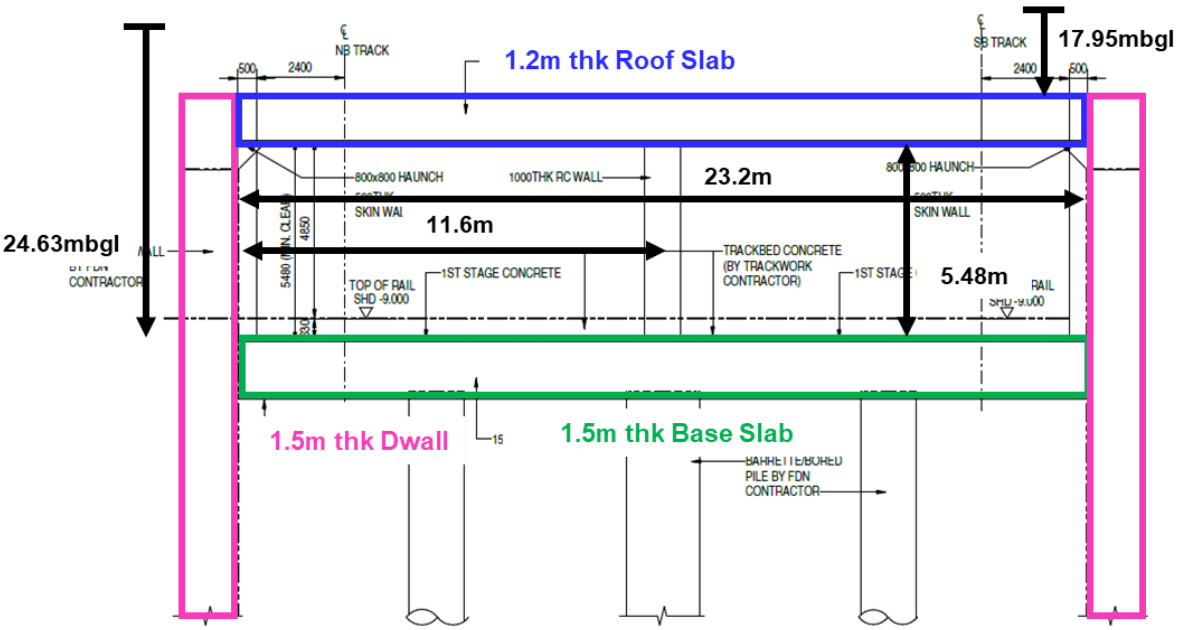

Figure A3. Typical cross section of C717 Cut-and-Cover Overrun Tunnel

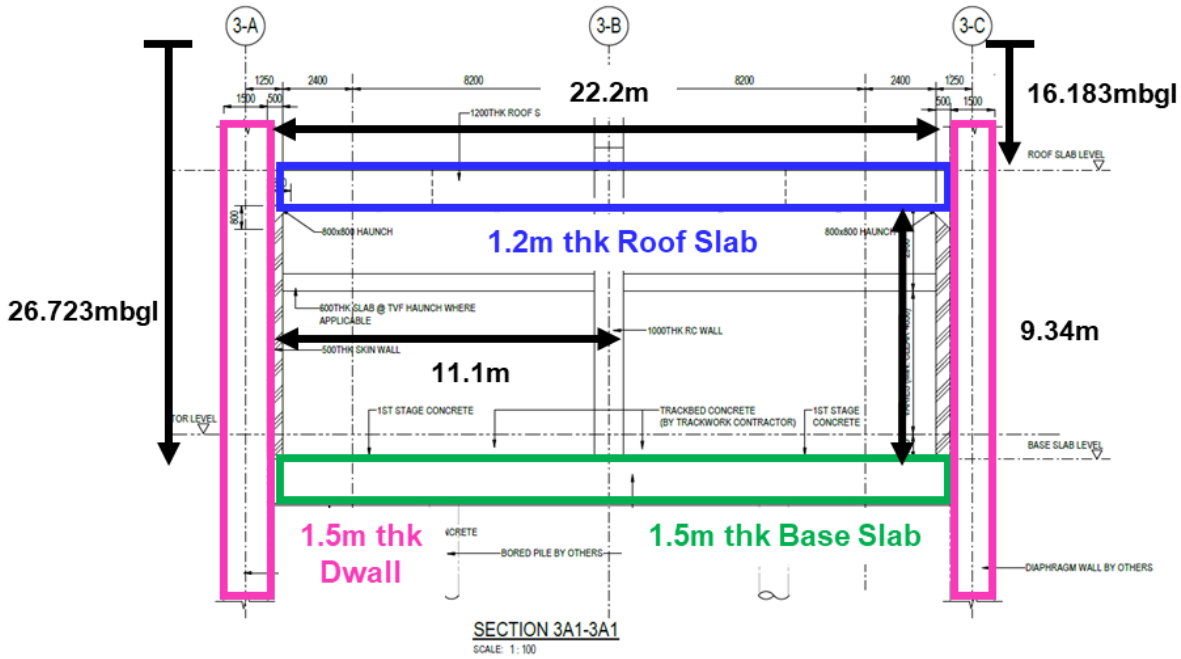

Figure A4. Typical cross section of C717 Cut-and-Cover Crossover Tunnel

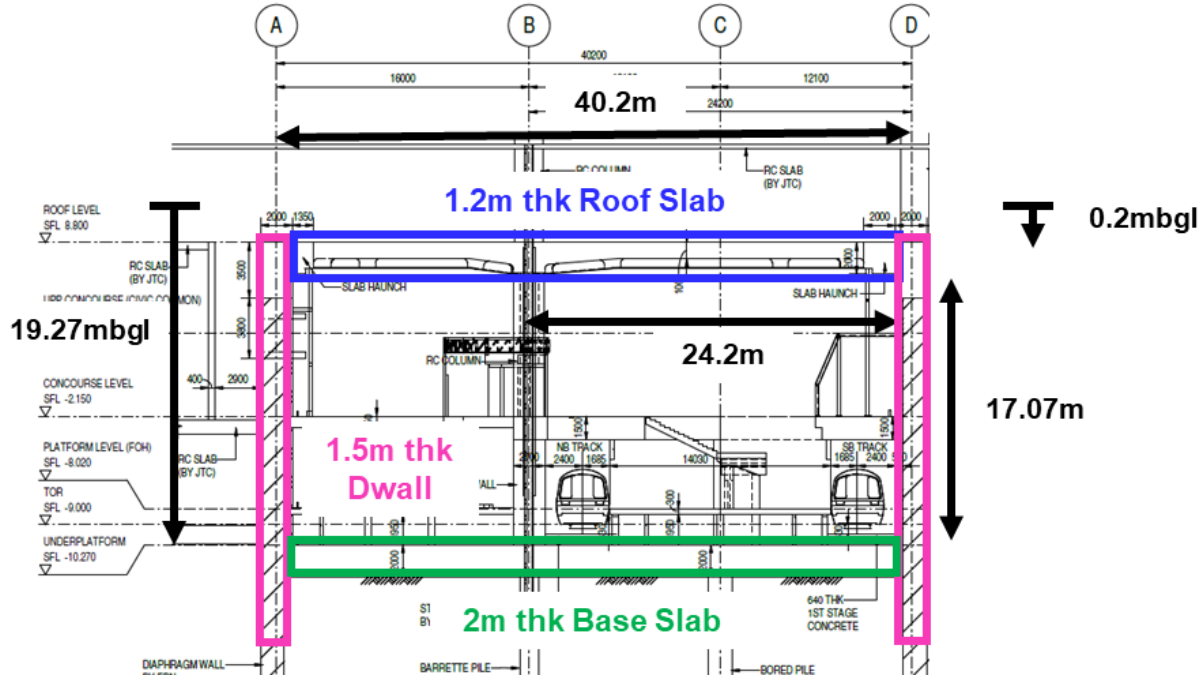

Figure A5. Typical cross section of NELe Punggol Coast Station

APPENDIX B

Location of design sections

Figures B1 to B5 show the location of all 51 design sections that were considered and re-designed:

- 15 design sections in the roof slab (RS)
- 16 design sections in the base slab (BS)
- 20 design sections in the diaphragm wall (DW)

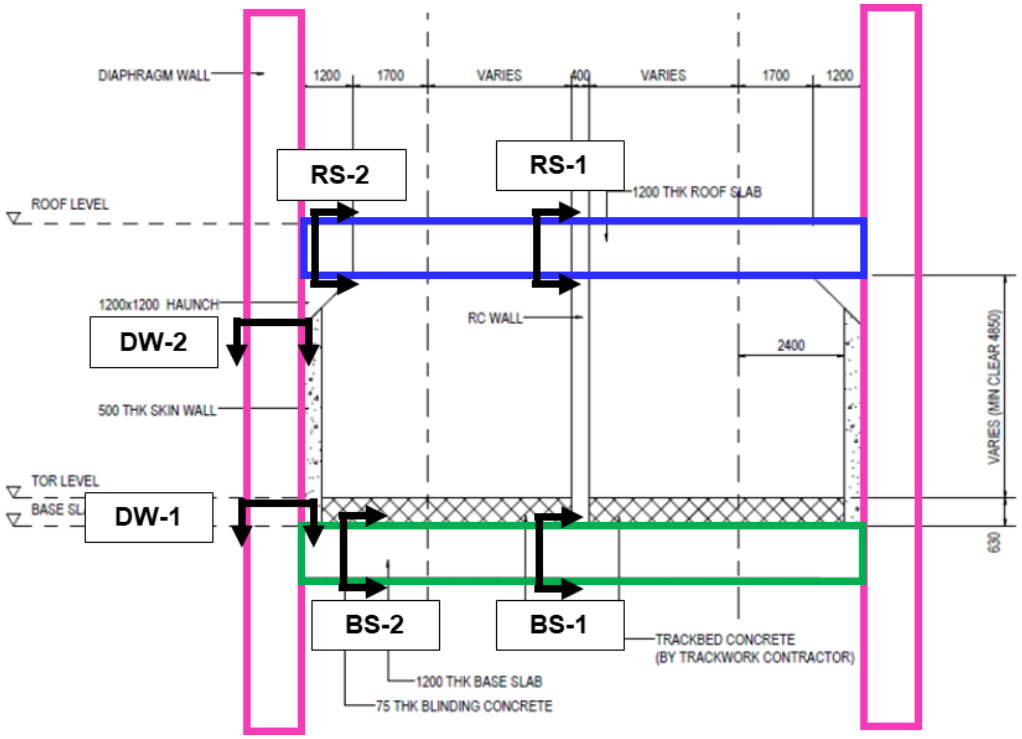

Figure B1. Location of design sections in C715 Cut-and-Cover Tunnel

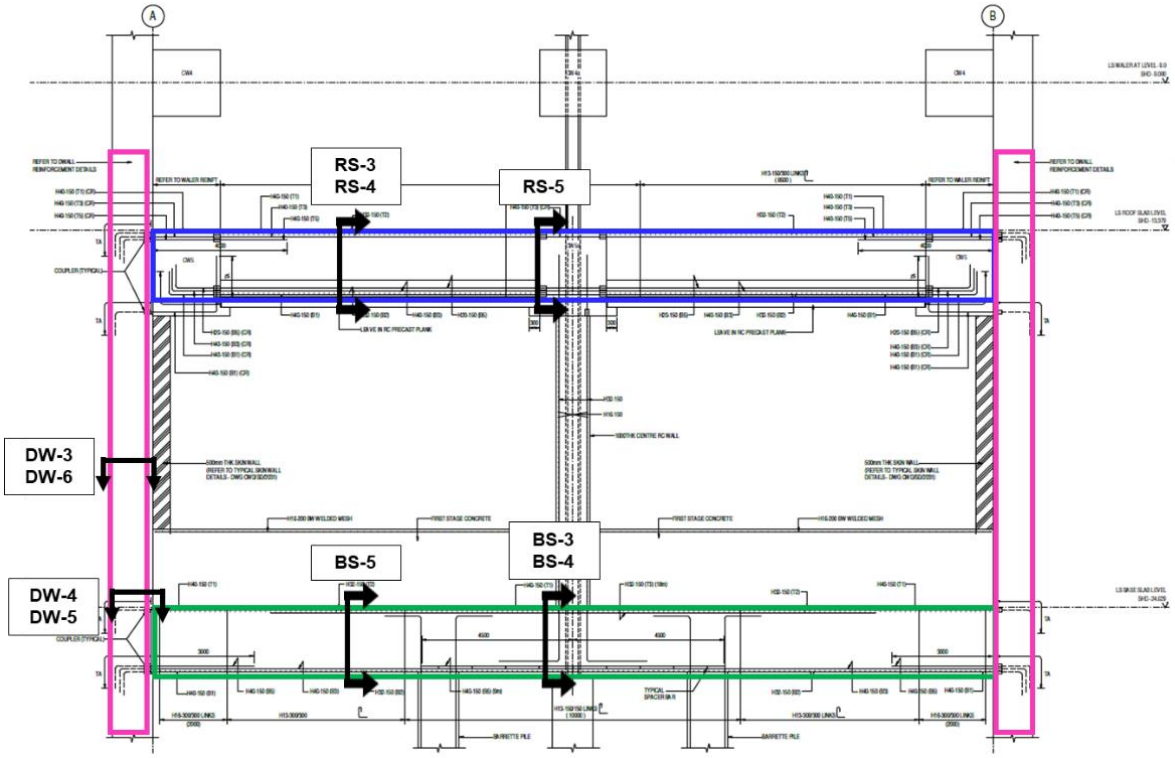

Figure B2. Location of design sections in TELe Cut-and-Cover Launch Shaft

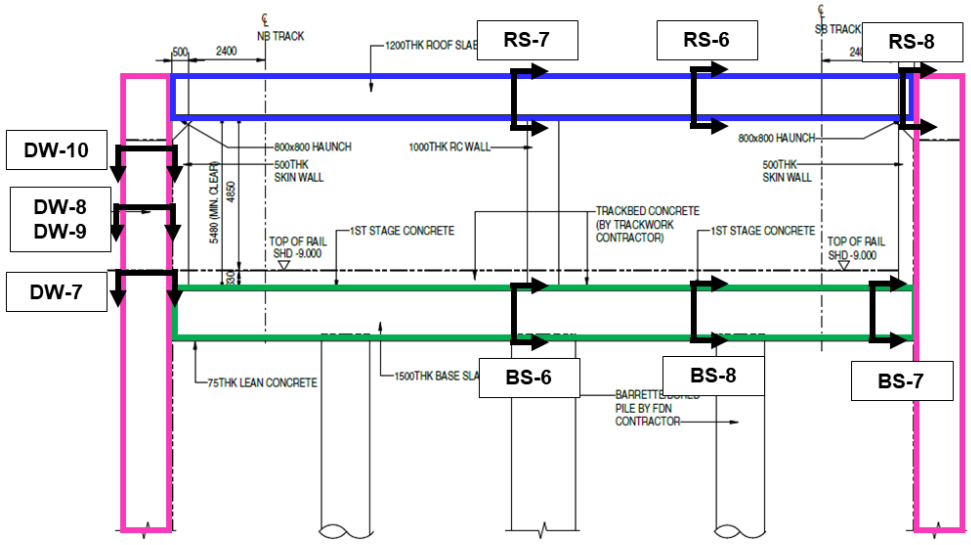

Figure B3. Location of design sections in C717 Cut-and-Cover Overrun Tunnel

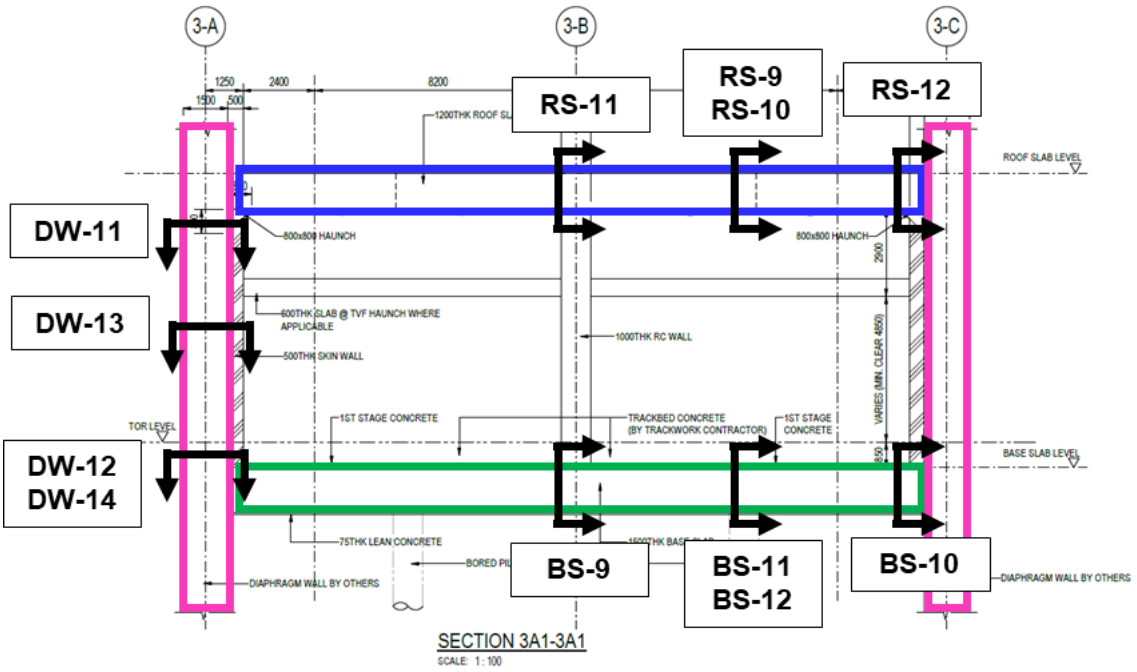

Figure B4. Location of design sections in C717 Cut-and-Cover Crossover Tunnel

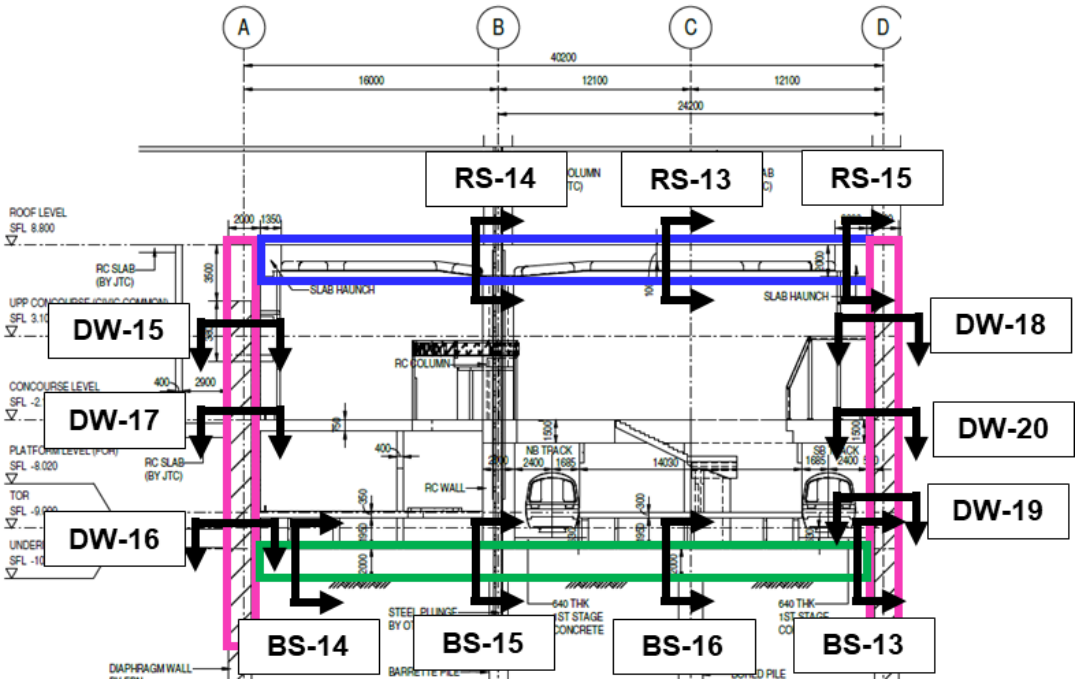

Figure B5. Location of design sections in NELe Punggol Coast Station

APPENDIX C

Combined effects of steel fibres and steel grade on SLS and ULS design checks

Table C1 recaps on the list of design scenarios that were considered. All the design sections were re-designed according to the Base DS, DS 1 and DS 4.

Table C2 summarises the results based on all case studies, and shows the combined effects of steel fibres and steel grade on SLS and ULS design checks for each design section and design scenario. For each design section, the most optimised design scenario that requires the minimum final rebar quantity is shaded in blue. The section number in Table C2 corresponds to the design section labels shown in Figures B1 to B5. It is also worth noting that two standard rebar spacings of 125mm and 150mm were considered for the re-design of section RS-1, BS-1 and DW-1. Subsequently, for all other design sections, a standard rebar spacing of 150mm is assumed to simplify the parametric study.

Table C1. Summary of design scenarios

Design Scenario (DS)	**Description**
Base DS	RC structure (f_{ck}=35 MPa) with rebar (f_{yk}=500 MPa) and without steel fibres
DS 1	Hybrid SFRC structure (f_{ck}=35 MPa) with rebar (f_{yk} =500 MPa) and steel fibres ($f_{R,1}$=3 MPa)
DS 4	Hybrid SFRC structure (f_{ck}=35 MPa) with rebar (f_{yk} =600 MPa) and steel fibres ($f_{R,1}$=3 MPa)

Table C2: Summary of results based on all case studies

Contract	Section Number	Section Thickness (mm)	ULS Design Moment (kNm)	SLS Design Moment (kNm)	Crack width limit (mm)	Design Scenario	ULS Rebar Quantity	ULS Bending Moment Capacity (kNm)	SLS Rebar Quantity	SLS Crack Width (mm)	Final Rebar Quantity
C715 C&C Tunnel	RS-1 (Roof Sagging)	1200	2000	1000	0.3	Base	H32-150	2493	H32-150	0.255	H32-150
						1	H32-150	2493	H25-150	0.218	H32-150
						4	H25-125	2182	H25-150	0.218	H25-125
C715 C&C Tunnel	RS-2 (Roof Hogging)	2400	3000	2000	0.25	Base	H40-150	3767	H32-150	Uncracked	H40-150
						1	H40-150	3767	H32-150	Uncracked	H40-150
						4	H40-150	4361	H32-150	Uncracked	H40-150
T316 Launch Shaft	RS-3 (Roof Sagging)	2000	7500	5400	0.3	Base	H40-150 H25-150	9026	H40-150 H40-150	0.277	H40-150 H40-150
						1	H40-150 H25-150	9026	H40-150 H25-150	0.202	H40-150 H25-150
						4	H40-150	7846	H40-150 H25-150	0.202	H40-150 H25-150
T316 Launch Shaft	RS-4 (Roof Hogging)	2000	2400	1800	0.25	Base	H25-150	2687	H25-150	Uncracked	H25-150
						1	H25-150	2687	H25-150	Uncracked	H25-150
						4	H25-150	3212	H25-150	Uncracked	H25-150
T316 Launch Shaft	RS-5 (Roof Hogging)	2000	9600	7100	0.25	Base	H40-150 H32-150	10445	H40-150 H40-150 H40-150 H25-150	0.236	H40-150 H40-150 H40-150 H25-150
						1	H40-150 H32-150	10445	H40-150 H32-150	0.235	H40-150 H32-150
						4	H40-150 H25-150	10521	H40-150 H32-150	0.235	H40-150 H32-150

Contract	Section Number	Section Thickness (mm)	ULS Design Moment (kNm)	SLS Design Moment (kNm)	Crack width limit (mm)	Design Scenario	ULS Rebar Quantity	ULS Bending Moment Capacity (kNm)	SLS Rebar Quantity	SLS Crack Width (mm)	Final Rebar Quantity
C717 Overrun	RS-6 (Roof Sagging)	1200	1510	1100	0.3	Base	H25-150	1549	H32-150	0.286	H32-150
						1	H25-150	1549	H25-150	0.241	H25-150
						4	H25-150	1846	H25-150	0.241	H25-150
C717 Overrun	RS-7 (Roof Hogging)	1200	2681	1966	0.25	Base	H40-150	3734	H40-150 H25-150	0.234	H40-150 H25-150
						1	H40-150	3734	H32-150	0.171	H40-150
						4	H32-150	2938	H32-150	0.171	H32-150
C717 Overrun	RS-8 (Roof Hogging)	2000	1398	1009	0.25	Base	H20-150	1733	H25-150	Uncracked	H25-150
						1	H20-150	1733	H25-150	Uncracked	H25-150
						4	H20-150	2075	H25-150	Uncracked	H25-150
C717 Crossover	RS-9 (Roof Sagging)	1200	1630	1180	0.3	Base	H32-150	2476	H40-150	0.178	H40-150
						1	H32-150	2476	H25-150	0.266	H32-150
						4	H25-150	1846	H25-150	0.266	H25-150
C717 Crossover	RS-10 (Roof Hogging)	1200	1300	900	0.25	Base	H25-150	1549	H32-150	0.209	H32-150
						1	H25-150	1549	H25-150	0.180	H25-150
						4	H25-150	1846	H25-150	0.180	H25-150
C717 Crossover	RS-11 (Roof Hogging)	1200	3103	2290	0.25	Base	H40-150	3734	H40-150 H32-150	0.241	H40-150 H32-150
						1	H40-150	3734	H40-150	0.207	H40-150
						4	H40-150	4401	H40-150	0.207	H40-150
C717 Crossover	RS-12 (Roof Hogging)	2000	4904	3535	0.25	Base	H40-150	6648	H40-150 H25-150	0.232	H40-150 H25-150
						1	H40-150	6648	H40-150	0.175	H40-150
						4	H32-150	5176	H40-150	0.175	H40-150

Contract	Section Number	Section Thickness (mm)	ULS Design Moment (kNm)	SLS Design Moment (kNm)	Crack width limit (mm)	Design Scenario	ULS Rebar Quantity	ULS Bending Moment Capacity (kNm)	SLS Rebar Quantity	SLS Crack Width (mm)	Final Rebar Quantity
C717 Station	RS-13 (Roof Sagging)	1000	2300	1630	0.3	Base	H40-150	3017	H40-150 H25-150	0.255	H40-150 H25-150
						1	H40-150	3017	H32-150	0.300	H40-150
						4	H32-150	2358	H32-150	0.300	H32-150
C717 Station	RS-14 (Roof Hogging)	1200	3650	2660	0.25	Base	H32-150	4380	H40-150 H25-150	0.165	H40-150 H25-150
						1	H32-150	4380	H32-150	0.214	H32-150
						4	H32-150	5146	H32-150	0.214	H32-150
C717 Station	RS-15 (Roof Hogging)	2000	4500	3160	0.25	Base	H40-150	6703	H40-150 H25-150	0.209	H40-150 H25-150
						1	H40-150	6703	H40-150	0.158	H40-150
						4	H32-150	5146	H40-150	0.158	H40-150

Contract	Section Number	Section Thickness (mm)	ULS Design Moment (kNm)	SLS Design Moment (kNm)	Crack width limit (mm)	Design Scenario	ULS Rebar Quantity	ULS Bending Moment Capacity (kNm)	SLS Rebar Quantity	SLS Crack Width (mm)	Final Rebar Quantity
C715 C&C Tunnel	BS-1 (Base Sagging)	1200	3000	2000	0.25	Base	H40-150	3754	H40-150 H25-150	0.250	H40-150 H25-150
						1	H40-150	3754	H40-150	0.183	H40-150
						4	H32-125	3450	H40-150	0.183	H40-150
C715 C&C Tunnel	BS-2 (Base Hogging)	1200	2000	2000	0.3	Base	H32-150	2493	H40-150 H16-150	0.299	H40-150 H16-150
						1	H32-150	2493	H40-150	0.183	H40-150
						4	H32-150	2915	H40-150	0.183	H40-150
T316 Launch Shaft	BS-3 (Base Sagging)	2000	14000	10200	0.25	Base	H40-150 H40-150 H25-150	14367	Comp: H40-150 Tension: H40-150 H40-150 H40-150 H40-150 H40-150	0.247	Comp: H40-150 Tension: H40-150 H40-150 H40-150 H40-150 H40-150
						1	H40-150 H40-150 H25-150	14367	H40-150 H40-150 H25-150	0.238	H40-150 H40-150 H25-150
						4	H40-150 H40-150	14387	H40-150 H40-150 H25-150	0.238	H40-150 H40-150 H25-150
T316 Launch Shaft	BS-4 (Base Hogging)	2000	2100	1900	0.3	Base	H25-150	2717	H10-150	uncracked	H25-150
						1	H25-150	2717	H10-150	uncracked	H25-150
						4	H25-150	3199	H10-150	uncracked	H25-150

Contract	Section Number	Section Thickness (mm)	ULS Design Moment (kNm)	SLS Design Moment (kNm)	Crack width limit (mm)	Design Scenario	ULS Rebar Quantity	ULS Bending Moment Capacity (kNm)	SLS Rebar Quantity	SLS Crack Width (mm)	Final Rebar Quantity
T316 Launch Shaft	BS-5 (Base Hogging)	2000	6100	3500	0.3	Base	H40-150	6714	H32-150 H32-150	0.256	H32-150 H32-150
						1	H40-150	6714	H32-150	0.292	H40-150
						4	H40-150	7859	H32-150	0.292	H40-150
C717 Overrun	BS-6 (Base Sagging)	1500	9840	7280	0.25	Base	H40-150 H40-150 H25-150	9935	Tension: H40-150 H40-150 H40-150 H40-150 H40-150 Comp: H40-150	0.240	Tension: H40-150 H40-150 H40-150 H40-150 H40-150 Comp: H40-150
						1	H40-150 H40-150 H25-150	9935	H40-150 H40-150	0.250	H40-150 H40-150 H25-150
						4	H40-150 H40-150	10005	H40-150 H40-150	0.250	H40-150 H40-150
C717 Overrun	BS-7 (Base Sagging)	1500	3536	2650	0.25	Base	H40-150	4860	H40-150 H32-150	0.215	H40-150 H32-150
						1	H40-150	4860	H40-150	0.190	H40-150
						4	H32-150	3752	H40-150	0.190	H40-150
C717 Overrun	BS-8 (Base Hogging)	1500	6544	4763	0.3	Base	H40-150 H32-150	7422	H40-150 H40-150 H32-150	0.285	H40-150 H40-150 H32-150
						1	H40-150 H32-150	7422	H32-150 H32-150	0.285	H40-150 H32-150
						4	H32-150 H32-150	6923	H32-150 H32-150	0.285	H32-150 H32-150

Contract	Section Number	Section Thickness (mm)	ULS Design Moment (kNm)	SLS Design Moment (kNm)	Crack width limit (mm)	Design Scenario	ULS Rebar Quantity	ULS Bending Moment Capacity (kNm)	SLS Rebar Quantity	SLS Crack Width (mm)	Final Rebar Quantity
C717 Crossover	BS-9 (Base Sagging)	1500	7355	5535	0.25	Base	H40-150 H32-150	7422	H40-150 H40-150 H40-150 H40-150	0.250	H40-150 H40-150 H40-150 H40-150
						1	H40-150 H32-150	7422	H40-150 H40-150	0.215	H40-150 H40-150
						4	H40-150 H25-150	7492	H40-150 H40-150	0.215	H40-150 H40-150
C717 Crossover	BS-10 (Base Sagging)	1500	5033	3757	0.25	Base	H32-150 H32-150	5963	H40-150 H32-150 H32-150	0.246	H40-150 H32-150 H32-150
						1	H32-150 H32-150	5963	H32-150 H32-150	0.216	H32-150 H32-150
						4	H40-150	5668	H32-150 H32-150	0.216	H32-150 H32-150
C717 Crossover	BS-11 (Base Sagging)	1500	1482	1046	0.25	Base	H25-150	1993	H10-150	Uncracked	H25-150
						1	H25-150	1993	H10-150	Uncracked	H25-150
						4	H20-150	1520	H10-150	Uncracked	H20-150
C717 Crossover	BS-12 (Base Hogging)	1500	4442	3309	0.3	Base	H40-150	4860	H40-150 H32-150	0.284	H40-150 H32-150
						1	H40-150	4860	H40-150	0.249	H40-150
						4	H40-150	5668	H40-150	0.249	H40-150

Contract	Section Number	Section Thickness (mm)	ULS Design Moment (kNm)	SLS Design Moment (kNm)	Crack width limit (mm)	Design Scenario	ULS Rebar Quantity	ULS Bending Moment Capacity (kNm)	SLS Rebar Quantity	SLS Crack Width (mm)	Final Rebar Quantity
C717 Station	BS-13 (Base Sagging)	2000	10900	8090	0.25	Base	H40-150 H40-150	12408	H40-150 H40-150 H40-150 H40-150	0.248	H40-150 H40-150 H40-150 H40-150
						1	H40-150 H40-150	12408	H40-150 H40-150	0.224	H40-150 H40-150
						4	H40-150 H32-150	12140	H40-150 H40-150	0.224	H40-150 H40-150
C717 Station	BS-14 (Base Sagging)	2000	5800	4580	0.25	Base	H40-150	6703	H40-150 H40-150	0.226	H40-150 H40-150
						1	H40-150	6703	H40-150	0.233	H40-150
						4	H40-150	7847	H40-150	0.233	H40-150
C717 Station	BS-15 (Base Sagging)	2000	8620	6910	0.25	Base	H40-150 H25-150	9026	H40-150 H40-150 H32-150 H32-150	0.237	H40-150 H40-150 H32-150 H32-150
						1	H40-150 H25-150	9026	H40-150 H32-150	0.228	H40-150 H32-150
						4	H32-150 H32-150	9711	H40-150 H32-150	0.228	H40-150 H32-150
C717 Station	BS-16 (Base Hogging)	2000	5100	2670	0.3	Base	H40-150	6703	H40-150	0.245	H40-150
						1	H40-150	6703	H32-150	0.203	H40-150
						4	H32-150	5146	H32-150	0.203	H32-150

Contract	Section Number	Section Thickness (mm)	ULS Design Moment (kNm)	SLS Design Moment (kNm)	Crack width limit (mm)	Design Scenario	ULS Rebar Quantity	ULS Bending Moment Capacity (kNm)	SLS Rebar Quantity	SLS Crack Width (mm)	Final Rebar Quantity
C715 C&C Tunnel	DW-1 (Dwall Sagging)	1200	6900	4000	0.3	Base	H40-150 H40-150 H25-150	6904	H40-150 H40-150 H32-150	0.287	H40-150 H40-150 H32-150
						1	H40-150 H40-150 H25-150	6904	H40-150 H40-150	0.262	H40-150 H40-150 H25-150
						4	H40-140 H40-150	7009	H40-150 H40-150	0.262	H40-150 H40-150
C715 C&C Tunnel	DW-2 (Dwall Hogging)	1200	4600	3200	0.25	Base	H40-140 H25-150	4700	H40-150 H40-150 H20-150	0.246	H40-150 H40-150 H20-150
						1	H40-140 H25-150	4700	H40-140 H32-150	0.242	H40-140 H32-150
						4	H40-140 H16-150	4698	H40-140 H32-150	0.242	H40-140 H32-150
T316 Launch Shaft	DW-3 (Dwall Sagging)	1200	6600	4850	0.3	Base	H40-150 H40-150 H20-150	6693	H40-150 H40-150 H40-150 H32-150	0.300	H40-150 H40-150 H40-150 H32-150
						1	H40-150 H40-150 H20-150	6693	H40-150 H40-150 H25-150	0.291	H40-150 H40-150 H25-150
						4	H40-150 H40-150	7043	H40-150 H40-150 H25-150	0.291	H40-150 H40-150 H25-150

Contract	Section Number	Section Thickness (mm)	ULS Design Moment (kNm)	SLS Design Moment (kNm)	Crack width limit (mm)	Design Scenario	ULS Rebar Quantity	ULS Bending Moment Capacity (kNm)	SLS Rebar Quantity	SLS Crack Width (mm)	Final Rebar Quantity
T316 Launch Shaft	DW-4 (Dwall Sagging)	1200	4350	3200	0.3	Base	H40-150 H25-150	4720	H40-150 H40-150	0.271	H40-150 H40-150
						1	H40-150 H25-150	4720	H40-150 H25-150	0.283	H40-150 H25-150
						4	H40-150 H13-150	4541	H40-150 H25-150	0.283	H40-150 H25-150
T316 Launch Shaft	DW-5 (Dwall Hogging)	1200	5250	4050	0.25	Base	H40-150 H32-150	5367	H40-150 H40-150 H32-150 H32-150	0.259	H40-150 H40-150 H32-150 H32-150
						1	H40-150 H32-150	5367	H40-150 H32-150 H20-150	0.288	H40-150 H32-150 H20-150
						4	H40-150 H25-150	5432	H40-150 H32-150 H20-150	0.288	H40-150 H32-150 H20-150
T316 Launch Shaft	DW-6 (Dwall Hogging)	1200	1000	890	0.25	Base	H25-150	1503	H32-150	0.169	H32-150
						1	H25-150	1503	H25-150	0.226	H25-150
						4	H20-150	1150	H25-150	0.226	H25-150
C717 Overrun	DW-7 (Dwall Hogging)	1500	4500	3500	0.25 0.25 0.25 0.25	Base	H40-150	4698	H40-150 H40-150	0.211	H40-150 H40-150
						1	H40-150	4698	H40-150 H25-150	0.228	H40-150 H25-150
						4	H40-150	5477	H40-150 H25-150	0.228	H40-150 H25-150

Contract	Section Number	Section Thickness (mm)	ULS Design Moment (kNm)	SLS Design Moment (kNm)	Crack width limit (mm)	Design Scenario	ULS Rebar Quantity	ULS Bending Moment Capacity (kNm)	SLS Rebar Quantity	SLS Crack Width (mm)	Final Rebar Quantity
C717 Overrun	DW-8 (Dwall Hogging)	1500	3600	2400	0.3	Base	H40-150	4698	H40-150	0.292	H40-150
						1	H40-150	4698	H40-150	0.211	H40-150
						4	H32-150	3630	H40-150	0.211	H40-150
C717 Overrun	DW-9 (Dwall Sagging)	1500	2800	1800	0.25	Base	H32-150	3097	H40-150	0.189	H40-150
						1	H32-150	3097	H32-150	0.238	H32-150
						4	H32-150	3629	H32-150	0.238	H32-150
C717 Overrun	DW-10 (Dwall Hogging)	1500	2400	1800	0.25	Base	H32-150	3097	H40-150	0.189	H40-150
						1	H32-150	3097	H32-150	0.238	H32-150
						4	H32-150	3629	H32-150	0.238	H40-150
C717 Crossover	DW-11 (Dwall Hogging)	1500	7000	4500	0.25	Base	H40-150 H32-150	7156	H40-150 H40-150 H32-150	0.23	H40-150 H40-150 H32-150
						1	H40-150 H32-150	7156	H40-150 H25-150 H25-150	0.246	H40-150 H25-150 H25-150
						4	H40-150 H25-150	7225	H40-150 H25-150 H25-150	0.246	H40-150 H25-150 H25-150
C717 Crossover	DW-12 (Dwall Hogging)	1500	4250	3000	0.25	Base	H40-150	4698	H40-150 H32-150	0.213	H40-150 H32-150
						1	H40-150	4698	H32-150 H32-150	0.206	H32-150 H32-150
						4	H40-150	4698	H32-150 H32-150	0.206	H32-150 H32-150

Contract	Section Number	Section Thickness (mm)	ULS Design Moment (kNm)	SLS Design Moment (kNm)	Crack width limit (mm)	Design Scenario	ULS Rebar Quantity	ULS Bending Moment Capacity (kNm)	SLS Rebar Quantity	SLS Crack Width (mm)	Final Rebar Quantity
C717 Crossover	DW-13 (Dwall Hogging)	1500	2000	1000	0.25	Base	H32-150	3097	H25-150	0.250	H32-150
						1	H32-150	3097	H25-150	0.185	H32-150
						4	H25-150	2269	H25-150	0.185	H25-150
C717 Crossover	DW-14 (Dwall Sagging)	1500	7400	4600	0.3	Base	H40-150 H40-150	8398	H40-150 H32-150 H32-150	0.271	H40-150 H32-150 H32-150
						1	H40-150 H40-150	8398	H32-150 H32-150 H20-150	0.297	H32-150 H32-150 H20-150
						4	H40-150 H32-150	8254	H32-150 H32-150 H20-150	0.297	H32-150 H32-150 H20-150
C717 Station	DW-15 (Left Dwall Hogging)	1500	4095	2778	0.25	Base	H40-150	4698	H40-150 H25-150	0.230	H40-150 H25-150
						1	H40-150	4698	H32-150 H25-150	0.238	H32-150 H25-150
						4	H40-150	5477	H32-150 H25-150	0.238	H32-150 H25-150
C717 Station	DW-16 (Left Dwall Hogging)	1500	6080	5000	0.25	Base	H40-150 H25-150	6238	H40-150 H40-150 H40-150	0.231	H40-150 H40-150 H40-150
						1	H40-150 H25-150	6238	H40-150 H40-150	0.244	H40-150 H40-150
						4	H32-150 H32-150	6678	H40-150 H40-150	0.244	H40-150 H40-150

Contract	Section Number	Section Thickness (mm)	ULS Design Moment (kNm)	SLS Design Moment (kNm)	Crack width limit (mm)	Design Scenario	ULS Rebar Quantity	ULS Bending Moment Capacity (kNm)	SLS Rebar Quantity	SLS Crack Width (mm)	Final Rebar Quantity
C717 Station	DW-17 (Left Dwall Sagging)	1500	6204	4584	0.3	Base	H40-150 H25-150	6238	H40-150 H40-150	0.296	H40-150 H40-150
						1	H40-150 H25-150	6238	H40-150 H32-150	0.267	H40-150 H32-150
						4	H32-150 H32-150	6678	H40-150 H32-150	0.267	H40-150 H32-150
C717 Station	DW-18 (Right Dwall Hogging)	1500	7727	5522	0.25	Base	H40-150 H40-150	8398	H40-150 H40-150 H32-150 H32-150	0.249	H40-150 H40-150 H32-150 H32-150
						1	H40-150 H40-150	8398	H40-150 H40-150 H25-150	0.236	H40-150 H40-150 H25-150
						4	H40-150 H32-150	8254	H40-150 H40-150 H25-150	0.236	H40-150 H40-150 H25-150
C717 Station	DW-19 (Right Dwall Hogging)	1500	7976	6299	0.25	Base	H40-150 H40-150	8398	H40-150 H40-150 H40-150 H32-150 H32-150	0.246	H40-150 H40-150 H40-150 H32-150 H32-150
						1	H40-150 H40-150	8398	H40-150 H40-150 H40-150	0.229	H40-150 H40-150 H40-150
						4	H40-150 H32-150	8254	H40-150 H40-150 H40-150	0.229	H40-150 H40-150 H40-150

Contract	Section Number	Section Thickness (mm)	ULS Design Moment (kNm)	SLS Design Moment (kNm)	Crack width limit (mm)	Design Scenario	ULS Rebar Quantity	ULS Bending Moment Capacity (kNm)	SLS Rebar Quantity	SLS Crack Width (mm)	Final Rebar Quantity
C717 Station	DW-20 (Right Dwall Sagging)	1500	4611	3451	0.3	Base	H40-150	4698	H40-150 H32-150	0.255	H40-150 H32-150
						1	H40-150	4698	H32-150 H32-150	0.248	H32-150 H32-150
						4	H40-150	5477	H32-150 H32-150	0.248	H32-150 H32-150